Original Research Paper

Cyclodextrin/chitosan nanoparticles for oral ovalbumin delivery: Preparation, characterization and intestinal mucosal immunity in mice

Muye He[b], Chen Zhong[b], Huibing Hu[b], Yu Jin[b], Yanzuo Chen[b], Kaiyan Lou[b,c], Feng Gao[a,b,c,]*

[a] *Shanghai Key Laboratory of Functional Materials Chemistry, East China University of Science and Technology, Shanghai 200237, China*
[b] *Department of Pharmaceutics, School of Pharmacy, East China University of Science and Technology, Shanghai 200237, China*
[c] *Shanghai Key Laboratory of New Drug Design, East China University of Science and Technology, Shanghai 200237, China*

ARTICLE INFO

ABSTRACT

A novel oral protein delivery system with enhanced intestinal penetration and improved antigen stability based on chitosan (CS) nanoparticles and antigen-cyclodextrin (CD) inclusion complex was prepared by a precipitation/coacervation method. Ovalbumin (OVA) as a model antigen was firstly encapsulated by cyclodextrin, either β-cyclodextrin (β-CD) or carboxymethyl-hydroxypropyl-β-cyclodextrin (CM-HP-β-CD) and formed OVA-CD inclusion complexes, which were then loaded to chitosan nanoparticles to form OVA loaded β-CD/CS or CM-HP-β-CD/CS nanoparticles with uniform particle size (836.3 and 779.2 nm, respectively) and improved OVA loading efficiency (27.6% and 20.4%, respectively). *In vitro* drug release studies mimicking oral delivery condition of OVA loaded CD/CS nanoparticles showed low initial releases at pH 1.2 for 2 h less than 3.0% and a delayed release which was below to 30% at pH 6.8 for further 72 h. More importantly, after oral administration of OVA loaded β-CD/CS nanoparticles to Balb/c mice, OVA-specific sIgA levels in jejunum of OVA loaded β-CD/CS nanoparticles were 3.6-fold and 1.9-fold higher than that of OVA solution and OVA loaded chitosan nanoparticles, respectively. *In vivo* evaluation results showed that OVA loaded CD/CS nanoparticles could enhance its efficacy for inducing intestinal mucosal immune response. In conclusion, our data suggested that CD/CS nanoparticles could serve as a promising antigen-delivery system for oral vaccination.

* Corresponding author at: Department of Pharmaceutics, School of Pharmacy, East China University of Science and Technology, 130 Meilong Road, Shanghai 200237, China, Tel.: +86 21 64258277.
E-mail address: fgao@ecust.edu.cn (F. Gao).
Peer review under responsibility of Shenyang Pharmaceutical University.

1. Introduction

Immunization has been widely used in clinic to cure transmissible diseases. Commercial proteins are commonly delivered through injection with poor patient compliance. Oral protein delivery provides alternative way for immunization with good compliance and elicits immune responses at mucosal surfaces of intestine, where membranous cells (M cells) exist for about 1 out of 10 million epithelial cells [1]. Large quantities of antigen could be possibly recognized by M cells non-specifically, and then be transferred across tight epithelial cells to reach b lymphocytes (B cells) at Peyer's Patches. Antigen be uptaken by Peyer's patches is an essential step in oral vaccination, it can induce both local and systemic immune response [2]. As M cells exist on mucosal surfaces of intestine, oral protein delivery is particularly suitable for inducing mucosal immunization. However, oral protein delivery faces major limitation of potential inactivation toward proteins. For example, proteins can be degraded by enzymes in gastrointestinal tract, and are unstable at low pH in stomach, which leads to lower oral bioavailability and further requirement of repeated administration of antigen [2]. Therefore, antigen protection, mainly protein protection, against inactivation factors such as low pH, enzyme, and bile salt, is the key to design oral protein delivery system. In the past, polymer nanoparticle-based delivery system made from polymethyl methacrylate, polyesters, polyamides, albumin, starch, chitosan, dextran, and etc. has shown to be promising for oral delivery of proteins [3], with some under consideration in clinical trials in Europe and United States [4]. There is still in great need of novel orally administered protein delivery system with improved antigen protection and immunization efficiency as well as safety [5].

One challenging problem associated with protein delivery is to overcome protein inactivation inside human body [6]. The possible reasons of protein inactivation include conformational change, covalent bond break, aggregation or precipitation [7]. Traditionally, additional excipients such as surfactant were added to prevent protein inactivation but causing adverse effect. For example, surfactant increases the rate of aggregation and drug oxidation and thus reduces shelf-time [7]. Therefore, novel excipients to protect protein from inactivation with fewer or no side effect are urgently needed. In this regards, both cyclodextrin (CD) and chitosan (CS) have emerged as new potential and promising excipients for increasing protein thermostability [8], inhibiting protein aggregation [9], and stabilizing protein against freeze-drying process [10]. The stabilizing effect of cyclodextrin can be rationalized by its structure, which consists of a hydrophilic outer surface and a hydrophobic central cavity. Protein residues from some amino acids such as phenylalanine, tyrosine, histidine, and tryptophan can be encapsulated in the cavity of cyclodextrin by non-covalent interactions, thus preventing protein aggregation without affecting its activity. Moreover, research also showed that cyclodextrin could inhibit the aggregation through retaining the tertiary structure of protein against denaturation induced by chemical factors or heat. Other researches indicated that cyclodextrin functions were similar to non-ionic surfactant for preventing protein degeneration.

In addition, it has been demonstrated that β-cyclodextrin (β-CD) can also improve drug stability [11] and acquire sustained release profile [12]. For the above reasons, in this study, we use β-CD as the essential part to establish inclusion complexes for oral protein delivery.

Besides from cyclodextrin, chitosan, a biodegradable, biocompatible natural polymer with good bio-adhesive properties, is also widely used in pharmaceutics [13–16]. Chitosan particles can improve the permeability of macromolecules through the epithelial tight junction and has shown in several reports to be able to encapsulate antigen and deliver to Peyer's Patches. For example, Lubben [17] prepared ovalbumin (OVA) loaded chitosan microparticles with higher loading efficiency by a precipitation/coacervation method, and the obtained chitosan microparticles could reach the Peyer's Patches according to in vivo experiment. In another report, Lubben [18] used chitosan microparticles for mucosal vaccination against diphtheria, and systemic as well as local immune responses were found in Balb/c mice. Moreover the drug could release from chitosan particulates in a controlled-release manner [19,20].

Therefore, we firstly reported a novel oral protein delivery system based on nanoparticles constructed from cyclodextrin and chitosan. OVA, a protein with 385 amino acids and relative molecular mass of 45 kDa [21], was used as the model antigen to form OVA-CD inclusion complexes firstly by the stirring-freeze-dried method. The OVA-CD inclusion complexes loaded chitosan nanoparticles were prepared by a precipitation/coacervation method. OVA loaded nanoparticles were characterized by in vitro property studies including particle size distribution, encapsulation efficiency, loading efficiency and in vitro drug release studies. OVA-specific secretory IgA (sIgA) levels in intestinal mucosal and IgG levels in serum were determined by enzyme-linked immunosorbent assay (ELISA) to study immune response in Balb/c mice.

2. Materials and methods

2.1. Chemicals, reagents and animals

Chitosan (Mw = 110 kDa, 90.0% deacetylation degree) was purchased from Yuhuan Ocean Biochemical Co. Ltd (Hangzhou, China). β-CD was purchased from Sinopharm Chemical Reagent Co. Ltd (Shanghai, China). Carboxymethyl-β-cyclodextrin (CM-β-CD) and hydroxypropyl-β-cyclodextrin (HP-β-CD) were purchased from Zhiyuan Biotech Co. Ltd. (Binzhou, China). Ovalbumin was purchased from Sigma Aldrich (Munich, Germany). The microBCA protein assay kit was supplied by Beyotime Institute of Biotechnology Co. Ltd (Shanghai, China). Mouse IgG and sIgA ELISA Quantitation Kits were purchased from Elabscience Biotechnology Co. Ltd (WuHan, China). All other reagents used in this study were high performance liquid chromatography (HPLC) or reagent grade.

Balb/c mice (20 ± 2 g) used in the experiments were supplied by the Department of Experimental Animals at Nanjing CAVENS biotechnology Co. Ltd (Nanjing, China). The animal experiments were carried out in accordance with the guidelines evaluated and approved by the ethics committee of East China University of Science and Technology.

2.2. Synthesis of carboxymethyl-hydroxypropyl-β-cyclodextrin (CM-HP-β-CD)

CM-HP-β-CD was synthesized as described in the reference with minor modifications [22]. Briefly, CM-β-CD (4.12 g) was dissolved in 100 ml sodium hydroxide (3%, w/w) in a round-bottomed flask equipped with a constant pressure funnel, a reflux condensing tube, and a thermograph. 1, 2-propylene oxide (86.5 mM) was added slowly into the flask over a period of about 2 h when reaction mixture was stirred in ice bath. After that, the reaction mixture was stirred at 25 °C for 24 h, then neutralized to pH 7 with hydrochloric acid followed by filtration. The filtrate was then dialyzed and freeze dried to obtain CM-HP-β-CD.

2.3. Characterization of CM-HP-β-CD

^{1}H NMR spectra of the CM-β-CD and CM-HP-β-CD were recorded on a Bruker AVANCE 400 spectrometer at 400 MHz using D_2O as the solvent. The chemical shifts were reported in parts per million (ppm) and were referenced to the residual water signal ($\delta = 4.70$ ppm). Fourier transformed infrared (FT-IR) analysis was performed on a Nicolet 6700 FT-IR spectrometer. CM-β-CD and CM-HP-β-CD samples were pressed with potassium bromide into a pellet before being placed in the sample cell.

2.4. Preparation and characterization of OVA-CD inclusion complexes

2.4.1. Preparation of OVA-CD inclusion complexes
OVA-CD inclusion complexes in different stoichiometric molar ratio were prepared by an aqueous solution-stirring method and then dried by lyophilization. Briefly, different amount of β-CD, CM-β-CD, HP-β-CD or CM-HP-β-CD was weighed and dissolved in phosphate buffered saline (PBS), then the calculated amount of OVA was mixed thoroughly into solution under magnetic stirring for certain time to establishing equilibrium. The OVA-CD solution was then freeze-dried and reserved for further study.

2.4.2. Binding strength of OVA-CD complexes: stability constant
UV spectra of OVA-CD inclusion complexes were obtained using an UV/VIS spectroscopy (TU-1800SPC) in the range from 250 to 400 nm. The stability constant (K_c) was calculated according to literature procedure [23]. The Kc was calculated as follows [24]:

$$1/\Delta A = 1/(\Delta \varepsilon Kc[OVA]_0[CD]_0) + 1/\Delta \varepsilon[OVA]_0 \tag{1}$$

Where ΔA represents for the difference of absorbance between inclusion complexes solution and OVA solution, [CD] represents for concentration of CD and [OVA] represents for concentration of OVA, Kc and $\Delta \varepsilon$ can be calculated by nonlinear least-squares regression analysis.

2.4.3. Stoichiometry determination of OVA-CD inclusion complexes
The stoichiometry of OVA-CD inclusion complexes was determined by Job's plot. OVA and cyclodextrin mixed solution samples were prepared by keeping the total concentration of both components constant ([OVA] + [CD] = 10 mM), while changing the molar ratio of cyclodextrin to OVA as following: 4, 6, 8, 10, 12, 20 and 40. The solutions were allowed stirring for 4 h at room temperature, and UV absorbance at 280 nm was measured for all samples and the UV absorbance differences ($\Delta A = A–A_0$) between each sample (A) and reference OVA sample (A_0, [OVA] = 10 mM) were calculated and plotted versus the molar ratio of CD/OVA. The ratio corresponds to the maximum value of ΔA was regarded as the stoichiometric ratio of the OVA-CD inclusion complex.

2.4.4. Molecular docking
The x-ray crystal structure of ovalbumin (PDB ID:1OVA) was retrieved from Protein Data Bank (www.rcsb.org), while the structure of β-CD was extracted from the crystal structure of β-CD complex obtained from Protein Data Bank (PDB ID:3CGT). The water molecules have been removed from the 1OVA.pdb crystal structure prior to docking study and hydrogen atoms were added to ovalbumin crystal structure. A single molecule β-CD structure was geometrically optimized using the semi-empirical PM3 method according to lecture [25]. The optimized single β-CD structure was then used as the ligand in all docking processes. Molecular docking of β-CD to the insulin model was carried out using the AutoDock v4.2 software package [26,27]. Gasteiger charges were computed for each of the molecules. The grid maps were prepared using a $40 \times 40 \times 40$ grid box with the distance between two grid points set at 0.375 Å centering on ovalbumin. All rotational bonds in β-CD were set free, while those of ovalbumin were held rigid. The docking studies were carried out using the empirical free energy function and applying the standard protocol of the Lamarckian Genetic Algorithm (LGA). A total of 100 independent docking runs were carried out for each docking processes with a maximum number of 27 000 generations, a mutation rate of 0.02, a crossover rate of 0.08 and an elitism value of 1. The final lowest docked energy conformation is then used for the next run with another β-CD and the docking studies were repeated until the maximum number of β-CD yield a positive binding free energy value.

2.4.5. SEM images of OVA-CD inclusion complexes
Morphological analysis of OVA-CD inclusion complexes was performed by JEM-6360 LV scanning electron microscope (SEM) (JASCO, Japan). Samples were weighted and placed on brass plate, and observed after plated with a thin layer of gold.

2.5. Preparation of OVA loaded CD/CS nanoparticles

Chitosan nanoparticles were prepared by a precipitation/coacervation method as described in the reference with minor modifications [18]. Briefly, to a 0.25% (w/v) chitosan glacial acetic acid solution, Tween-80 was added to a final concentration of 1%. Then, sodium sulfate solution (10%, w/v, 0.2 ml) was added dropwise to the chitosan solution with magnetic stirring and ultrasonic for 30 min to form chitosan nanoparticles.

OVA loaded chitosan nanoparticles and CD/CS nanoparticles were prepared by the following procedure. Briefly, chitosan nanoparticles were resuspended in PBS solution, then

OVA or OVA-CD (β-CD or CM-HP-β-CD) inclusion complexes was added into the solution at 25 °C with stirring at 50 rpm for 3 h. The nanoparticle solution was freeze-dried to obtain dry nanoparticles.

2.6.　Morphological characterization of OVA loaded CD/CS nanoparticles

The particle size and zeta potential of chitosan nanoparticles in aqueous solution were measured using Delsa Nano dynamic light scattering (DLS) (Beckman Coulter Inc, USA) equipped with 4 mW He-Ne laser at a wave length of 633 nm at room temperature. The morphological evaluation of OVA loaded CM-HP-β-CD/CS nanoparticles was performed with transmission electron microscope (TEM). TEM images were taken on JEM-2010 (JEOL, Japan). The sample was stained with 2% (w/v) phosphotungstic acid before dropped on a copper grid.

2.7.　Entrapment efficiency, loading efficiency and stability study

To determine OVA entrapment and loading efficiency, OVA loaded CD/CS nanoparticles were centrifuged after preparation and the supernatant was collected. The concentration of OVA in supernatant was determined by microBCA according to supplier's instructions. The entrapment efficiency (EE) and loading efficiency (LE) were calculated as follows:

Entrapment efficiency (%)

$$= \frac{\text{total amount of OVA} - \text{free amount of OVA}}{\text{total amount of OVA}} \times 100\% \quad (2)$$

Loading efficiency (%)

$$= \frac{\text{total amount of OVA} - \text{free amount of OVA}}{\text{weight of nanoparticles}} \times 100\% \quad (3)$$

The chitosan nanoparticles, OVA loaded CS nanoparticles and OVA loaded CD/CS nanoparticles were freshly prepared at pH 6.0 with optimized reaction condition and preserved at 4 °C. Samples were collected at different time points up to one month. The size distribution of nanoparticles was measured by DLS. The stability of chitosan nanoparticles and OVA loaded CS nanoparticles were also investigated at pH 1.2 at room temperature for 2 h.

2.8.　In vitro drug release of OVA loaded CD/CS nanoparticles

The *in vitro* drug release from the OVA loaded CS nanoparticles and OVA loaded CD/CS nanoparticles were studied in solution sequentially at pH 1.2 and pH 6.8 to simulate the pH environment in the fasting stomach and then the small intestine. Briefly, the prepared nanoparticles were resuspended in solution at a concentration of 0.1% (w/v), then the solution was incubated in 37 °C at 100 rpm. After shaken for 0.5, 1 and 2 h at pH 1.2, and then 0.5, 1, 2, 4, 8, 12, 24, 48 and 72 h at pH 6.8 in the vessel, a 200 μl aliquot was sampled and refilled with an equal volume of fresh medium correspondingly. Each aliquot

sample was then centrifuged (10 000 rpm for 5 min) in a plastic tube to separate the supernatant for further determination of released OVA concentration in supernatant by microBCA assay.

2.9.　In vivo immunization experiments and determination of serum IgG and siga

Twenty male Balb/c mice were randomly divided into five groups, which were treated with OVA solution, OVA loaded CS nanoparticle, OVA loaded β-CD/CS nanoparticle, OVA loaded CM-HP-β-CD/CS nanoparticle and saline as control group. OVA containing solutions were prepared by dissolving the OVA or OVA loaded nanoparticles in PBS (w/v, 200 μg OVA-equivalent) and were administered after fasting for 24 h to mice orally (0.2 ml/mouse) for immunization [28]. Each mouse received immunization on day 0 and day 7 with different OVA formulations shown above. The immunization dosage on day 7 was doubled to ensure positive immune response. Blood samples (200 μl) were taken from the orbital sinus on day 14 and day 21, and the serum was isolated by centrifugation (10 000 rpm, 4 °C) and stored at −20 °C for IgG level analysis. The mice were then sacrificed after the blood samples were taken on day 21, then 5 cm of jejunum or ileum was cut as samples, supernatant was collected to test the OVA-specific sIgA by tissue homogenation, centrifugation (10 000 rpm, 4 °C) and stored at −20 °C until sIgA levels in intestine was analyzed. The OVA-specific IgG in serum and OVA-specific sIgA were examined by ELISA according to supplier's instructions.

2.10.　Statistical analysis

Multiple group comparisons were conducted using one-way analysis of variance (ANOVA). All data analysis was executed using the IBM SPSS Statistics 17.0. All data were presented as a mean value with its standard deviation indicated (mean ± SD). P-values less than 0.05 were considered to be statistically significant.

3.　Results and discussion

3.1.　Synthesis and characterization of CM-HP-β-CD

Fig. 1A included the ^{1}H NMR spectrum and the complete peak assignments for the CM-β-CD. The solvent peak of D$_2$O was found at 4.79 ppm. The peaks at 5.07 ppm and 3.40–4.30 ppm were assigned to the protons of carbon1-6 in β-CD segments, respectively. The peaks at 5.28 ppm were attributed to -CH$_2$- of the carboxymethyl (CM) group in CM-β-CD. Compared with CM-β-CD, characteristic peak of CM-HP-β-CD at δ (ppm) = 1.13–1.15 (methyl group(-CH$_3$) in hydroxypropyl (HP)) (Fig. 1B) was observed, suggested that HP had been introduced to CM-β-CD. It could be calculated from ^{1}H NMR integration that average molar substitution of HP and CM was 2.9 and 5.7, respectively. The FTIR spectra of CM-β-CD and CM-HP-β-CD are shown in Fig. 1C. The strong absorption peaks at 1594 cm^{-1}, 1419 cm^{-1}, and 1328 cm^{-1} were from ether group, and absorption at 3440 cm^{-1} was due to the alcoholic hydroxyl group in the CM-β-CD. In the IR spectrum of CM-HP-β-CD, the
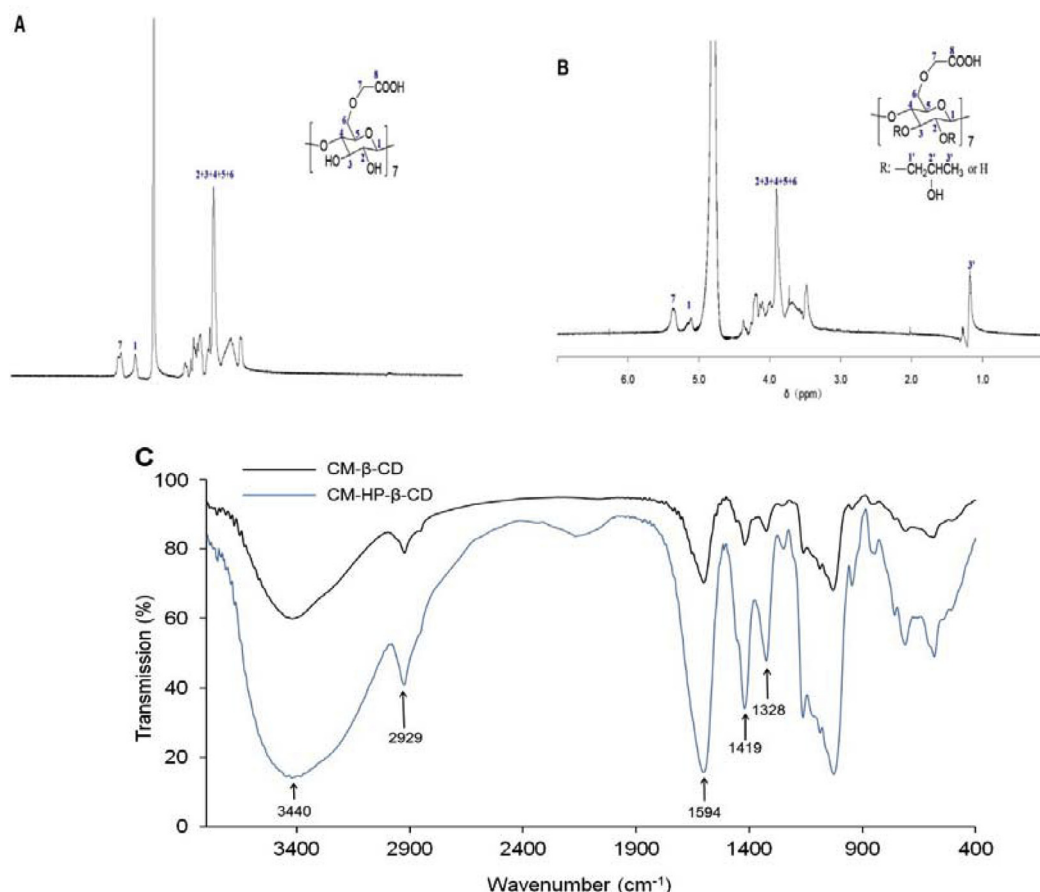
Fig. 1 – The ^{1}H NMR spectrum of CM-β-CD (A) and CM-HP-β-CD (B) and FT-IR spectrum of CM-β-CD and CM-HP-β-CD (C).

intensity of C–H stretch band at 2929/cm^{-1} increased, which could be attributed to the methylene group in the CM side chain. Evidences from ^{1}H NMR and IR spectra demonstrated the successful synthesis of CM-HP-β-CD.

3.2. Characterization of OVA-CD inclusion complexes

The OVA-CD inclusion complexes were prepared by the stirred-freeze-drying method. UV spectra (250 to 400 nm) were measured at different molar ratio of OVA to cyclodextrin (Fig. 2). The decrease of the ratio OVA/cyclodextrin was accompanied with increase of UV absorbance at around 280 nm, suggesting that increased amount of inclusion complex was formed between aromatic amino acid residues of OVA and cyclodextrin molecules. The stability constants (K_c values) of OVA-CD inclusion complexes are summarized in Table 1. K_c values of CM-β-CD and HP-β-CD could not be obtained by this method due to too small UV absorbance differences at various OVA to cyclodextrin ratios (Fig. 2B and C), which suggested that CM-β-CD and HP-β-CD have low binding efficiency with OVA. As β-CD and CM-HP-β-CD bound to OVA more strongly, they were selected to prepare OVA-CD inclusion complexes for further studies.

The stoichiometry of complex formation between OVA and either β-CD or CM-HP-β-CD was also determined. As shown in Fig. 3A and B, when the molar ratio of cyclodextrin to OVA

Table 1 – The results of Kc between OVA and cyclodextrin in the PBS buffer.

Cyclodextrin	Linear equation	R^2	Kc (M^{-1})
β-CD	Y = 0.0018X + 6.2444	0.9610	3.5×10^3
CM-β-CD	N.A	N.A	N.A
HP-β-CD	N.A	N.A	N.A
CM-HP-β-CD	Y = 0.0053X + 109.74	0.9991	2.1×10^4

Note: N.A: not available. Kc: stability constants.

reached 10, it reached the maximum absorbance difference, which indicates formation of 1:10 inclusion complexes between OVA and β-CD or CM-HP-β-CD. The molecular docking study was performed and the 3D structure of the OVA-β-CD formation with binding sites is shown in Fig. 3C. The interaction between conformation of OVA and β-CD at binding sites was analyzed by PyMOL. The docking results indicate that the 1:9 OVA/β-CD formation produces the most stable conformation in which β-CD form hydrophobic interactions with a total of 9 amino acids that are Asn86, Lys89, Lys186, Glu196, Glm226 and Trp274 on chain A, Lys58, Glu89 and Tyr94 on chain B. This result is in agreement with the result of stoichiometry of complex formation.
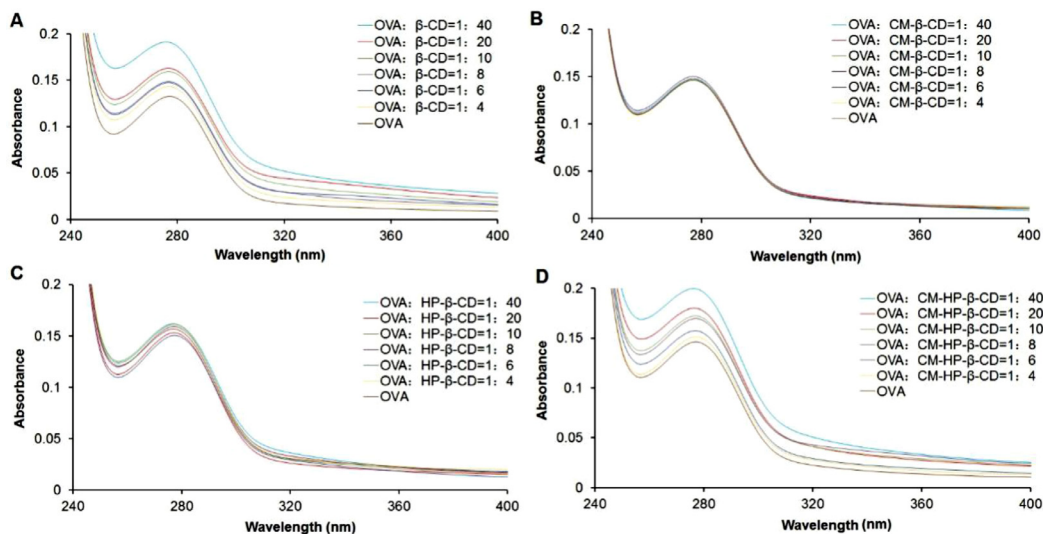
Fig. 2 – UV-VIS spectra of OVA and β-CD (A), CM-β-CD (B), HP-β-CD (C) and CM-HP-β-CD (D) at different molar ratio of OVA/cyclodextrin.
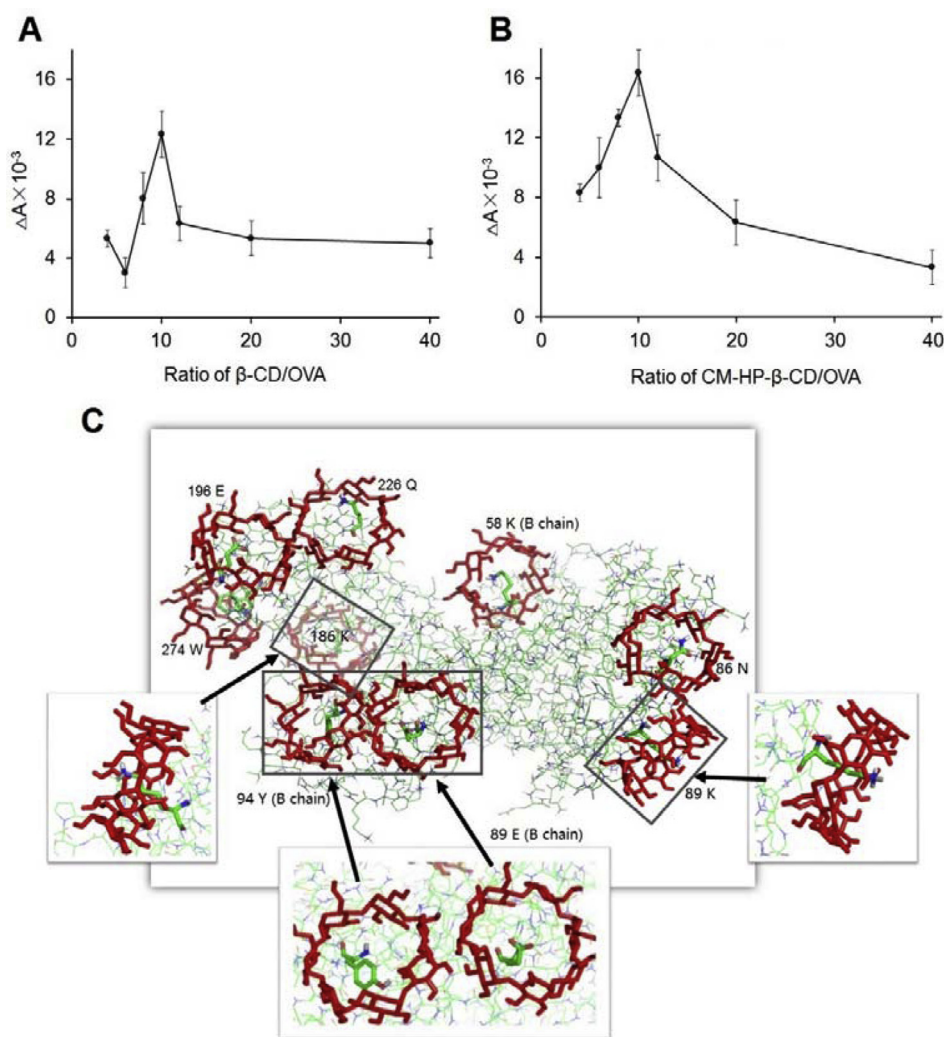

Fig. 3 – Changes of the difference in the absorbance as the ratio of β-CD/OVA (A) and CM-HP-β-CD/OVA (B). The 3D structure of OVA-β-CD inclusion complex formation that indicates nine β-CD molecule (red structure) binding on one OVA molecule (green structure) (C).
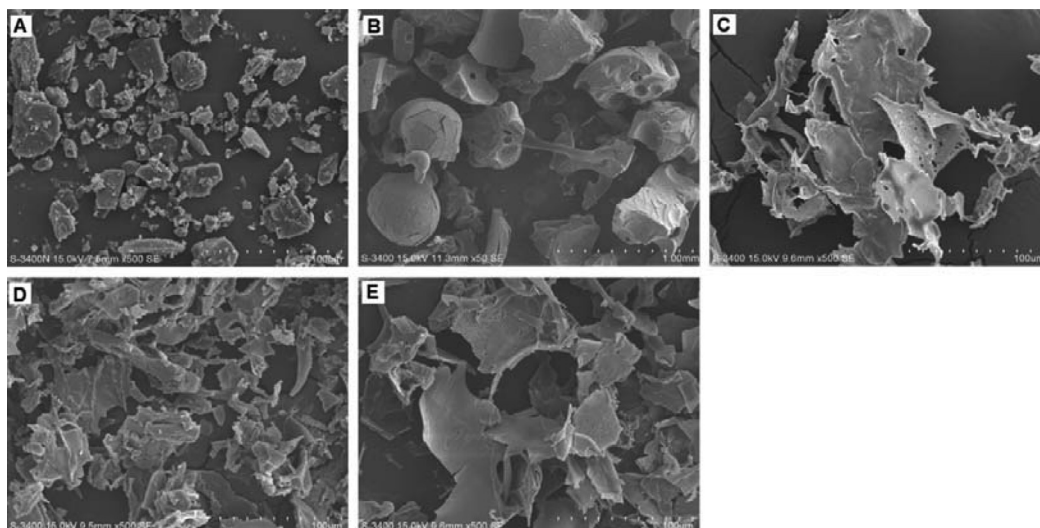
Fig. 4 – The SEM photographs of β-CD (A), CM-HP-β-CD (B), OVA (C), OVA-β-CD inclusion complex (D) and OVA-CM-HP-β-CD inclusion complex (E).
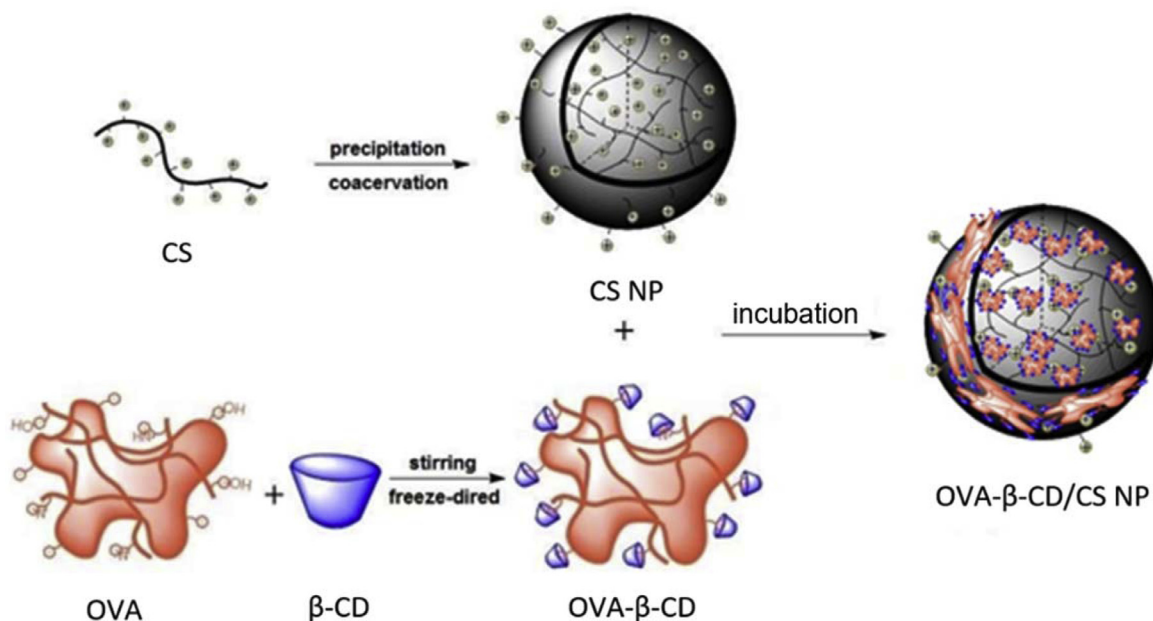

Fig. 5 – The possible formulation mechanism of OVA loaded β-CD/CS nanoparticles.

The SEM images showed morphology of OVA, β-CD, CM-HP-β-CD, OVA-β-CD inclusion complex, and OVA-CM-HP-β-CD inclusion complex (Fig. 4). SEM images OVA-CD inclusion complexes (Fig. 4D and E) presented both characteristics of OVA (Fig. 4C) and the cyclodextrin that they were derived (Fig. 4A and B), suggesting OVA was successfully encapsulated.

Interestingly, UV/Vis spectra of inclusion complexes (Fig. 2) showed the maximum absorption peak of OVA-CD inclusion complexes around 280 nm red-shifted slightly with increasing amount of cyclodextrin. This can be concluded that the increasing amount of cyclodextrin coupling on the surface of OVA, leading to an increased shielding effect on the amino acid residue of the protein [29].

3.3. Preparation and characterization of CD/CS nanoparticles

Several series of chitosan nanoparticles were prepared at different conditions by a precipitation/coacervation method and optimized by single-factor method. Encapsulation efficiency (EE) and loading efficiency (LE) were then investigated by microBCA. The optimized loading efficiency of OVA loaded nanoparticles of CS, β-CD/CS, and CM-HP-β-CD/CS were 30.9%, 27.6% and 20.4%, respectively, and the corresponding particle sizes were 213.6, 836.3 and 779.2 nm, respectively. Compared with the OVA-loaded chitosan nanoparticles, the size of OVA-loaded CD/CS nanoparticles increased signifi-
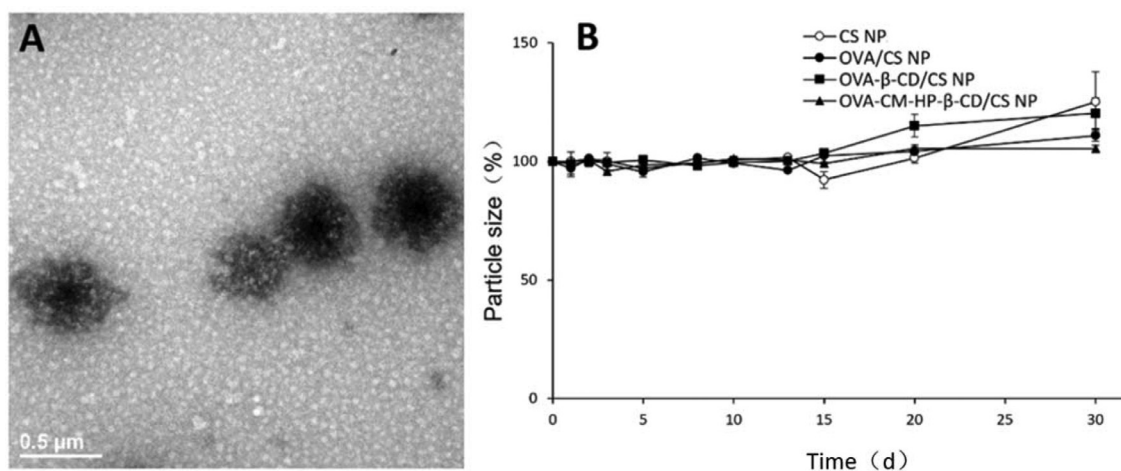
Fig. 6 – TEM photograph of the OVA loaded β-CD/CS nanoparticles (A). Size changes in CD/CS nanoparticles during one month-storage at pH 6.0 at 4 °C in PBS (B) (n = 3).
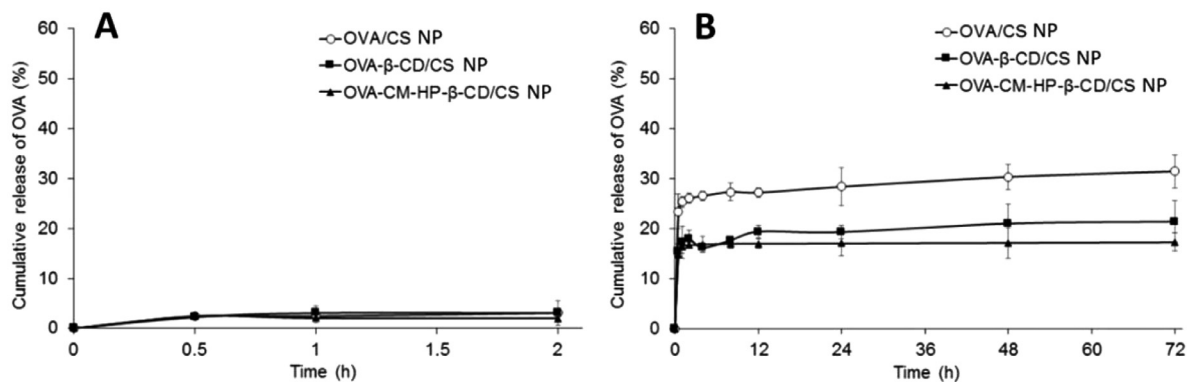

Fig. 7 – *In vitro* release of OVA from OVA loaded CS nanoparticles and OVA loaded CD/CS nanoparticles in PBS at pH 1.2 (A) and at pH 6.8 (B) at 37 °C (n = 3).

cantly. It can be speculated that during the preparation process, some of the OVA complex bound to the outer surface of particles, and particles aggregated together through protein and form a stable structure of nanoparticles. The possible mechanism in formation of OVA loaded CD/CS nanoparticles was illustrated in Fig. 5. The TEM image in Fig. 6A showed the spherical and uniform morphology of the OVA loaded β-CD/CS nanoparticles.

3.4. Stability study

The time-dependent stability of chitosan nanoparticles, OVA loaded CS nanoparticles, OVA loaded β-CD/CS nanoparticles and OVA loaded CM-HP-β-CD/CS nanoparticles was investigated at 4 °C, and particle size was measured in specific time points by DLS analysis as shown in Fig. 6B. No significant particle size changes of chitosan nanoparticles, OVA loaded CS nanoparticles and OVA loaded CM-HP-β-CD/CS nanoparticles were observed up to 30 d, indicating that all these nanoparticles were stable within 30 d. The small amount of increase

in the particle size of OVA loaded β-CD/CS nanoparticles after 20 d was acceptable, which may be caused by shielding effect of β-CD leading to lower electrostatic force between amino acid residue and chitosan. Moreover, we test the residual percent of OVA in CD/CS nanoparticles, 93.7% of OVA was retained in nanoparticles on day 30. The results suggested that OVA loaded chitosan nanoparticles were more stable than chitosan nanoparticles without OVA in acidic medium, likely due to stabilization effect of protein corona through OVA coated on the surface of nanoparticles by electrostatic interaction, which can protect chitosan from degradation by gastric acid.

3.5. In vitro drug release of OVA loaded CD/CS nanoparticles

The *in vitro* drug release profiles of OVA loaded CD/CS nanoparticles were investigated in solution at pH 1.2 for 2 h and pH 6.8 for 72 h sequentially at 37 °C to simulate the pH environment of the fasting stomach and then the small intestine
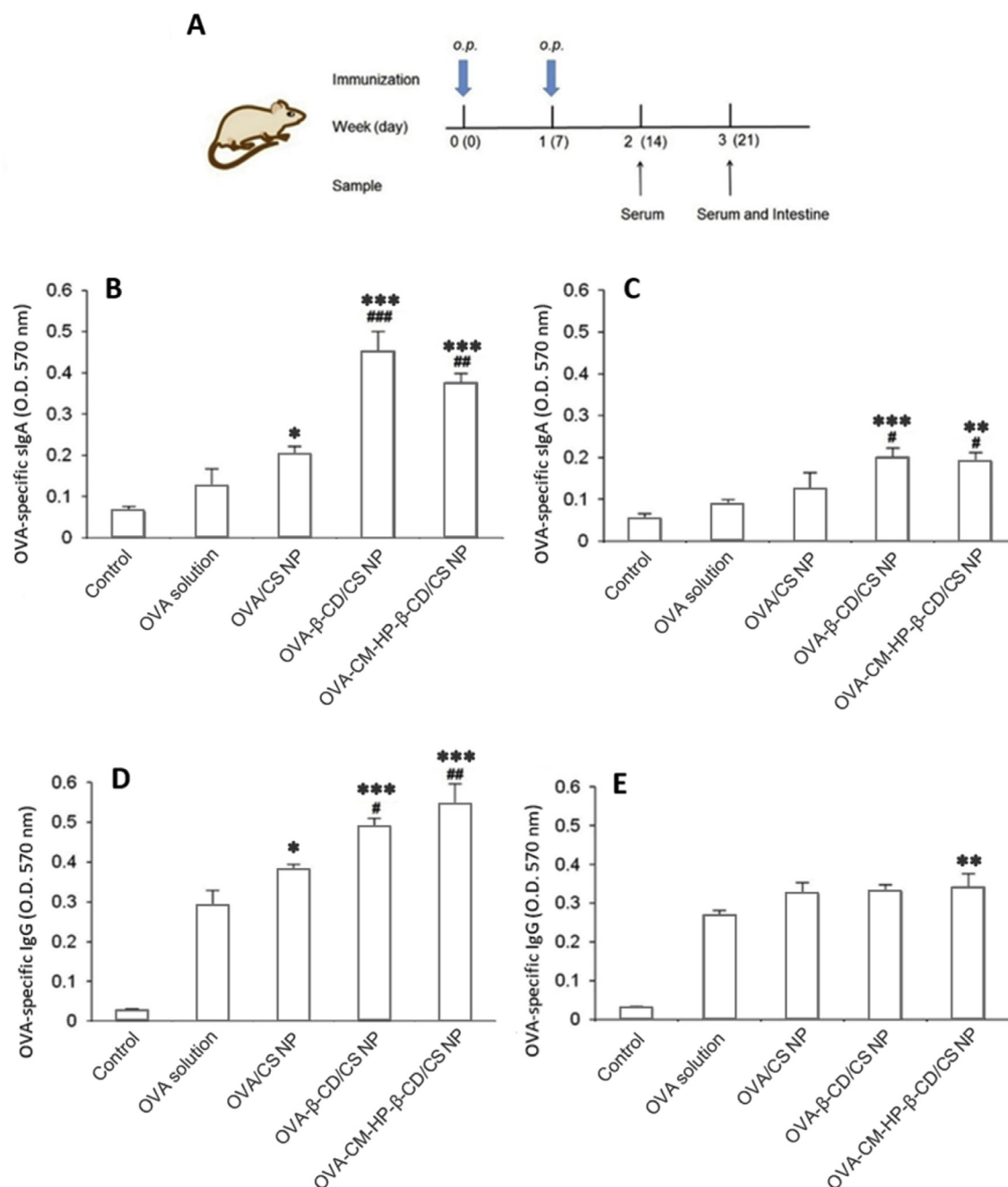
Fig. 8 – Schematic diagram of mice immunization with OVA loaded CD/CS nanoparticles (A). The level of OVA-specific sIgA in jejunum (B) and ileum (C) mucosa 21 d, and mouse OVA-specific IgG in serum 14 d (D) and 21 d (E), after the first time orally given OVA-loaded nanoparticles (n = 4). *$P < 0.05$, ** $P < 0.01$, *** $P < 0.001$ compared with OVA solution; # $P < 0.05$, ## $P < 0.01$, ### $P < 0.001$ compared with OVA loaded CS nanoparticles.

(Fig. 7). Both OVA loaded CS nanoparticles and OVA loaded CD/CS nanoparticles had similar sustained release profile in both pH environment, which showed an initial burst in the first hour likely due to desorption of the OVA on the surface of chitosan nanoparticles, followed by a delayed release. The total amount of OVA released from the OVA loaded CS nanoparticles and OVA loaded CD/CS nanoparticles were less than 3% within 2 h at pH 1.2, indicating that most of OVA protein molecules were loaded deep inside nanoparticles that

can keep OVA survived in the initial 2 h in the fasting stomach *in vivo*. Therefore, the relative low initial burst release at pH 1.2 is a favored property for oral immunization. In the following 72 h at pH 6.8, the amount of OVA released from the OVA loaded CS nanoparticles, OVA loaded β-CD/CS nanoparticles and OVA loaded CM-HP-β-CD/CS nanoparticles was 31.5%, 21.4% and 17.3%, respectively, indicating that incorporation of cyclodextrin in nanoparticles efficiently slowed down the rate of OVA release. This phenomenon

could be rationalized by stronger encapsulation of OVA inside nanoparticles through formation of OVA-CD inclusion complexes.

3.6. In vivo immune responses

The OVA-loaded nanoparticles were administered orally to Balb/c mice (Fig. 8A). OVA-specific IgG levels in serum and sIgA levels in intestinal were determined by ELISA. As shown in Fig. 8B and C, compared with the mice group treated with OVA solution, the OVA loaded CD/CS nanoparticle and OVA loaded CS nanoparticle mice groups had increased OVA-specific IgG level in serum after oral administration for 14 and 21 d The OVA-specific IgG levels increased more significantly on day 14 with about 1.3-fold, 1.7-fold and 1.9-fold increase for OVA loaded CS, β-CD/CS, and CM-HP-β-CD/CS nanoparticle treated mice group, respectively. The results indicated that chitosan-derived nanoparticles could enhance the bioavailability of OVA at small intestine, likely caused by protection of OVA from inactivation due to low pH and enzymes in the gastrointestinal tract. The results were also in agreement with literature [30,31]. The elevated level of IgG was also observed for the OVA loaded CS and CD/CS nanoparticle treated groups compared with the OVA solution group at statistically significant level on day 21 ($P < 0.05$).

In Fig. 8D and E, elevated OVA-specific sIgA level was also found in OVA-loaded nanoparticle groups. Compared with the OVA solution group, OVA-specific sIgA level in jejunum of the OVA-loaded CS, β-CD/CS, and CM-HP-β-CD/CS nanoparticle treated groups increased about 1.9-fold, 3.6-fold and 3.0-fold on day 21, respectively. The corresponding values in ileum on day 21 were 1.4-fold, 2.3-fold and 2.1-fold, respectively, which are in accordance with previous research [31]. Moreover, the higher level of OVA-specific sIgA observed in jejunum than in ileum was likely caused by the phagocytosis of M-cells mainly occurred in jejunum and thus produced a higher level of OVA-specific sIgA [32]. Besides, increased sIgA level in groups of mice treated with nanoparticles with cyclodextrin in both jejunum and ileum clearly shows the synergetic effect of cyclodextrin and chitosan. It is reported that cyclodextrins have no effect on the oral administration of proteins and neither have any promising effects as adjuvants [33]. Here, cyclodextrin probably function as stabilizer to protect the loaded protein from acidic and enzymatic degradation in the gastrointestinal tract through formation of inclusion complex. The results showed OVA loaded CD/CS nanoparticles exhibited a more delayed OVA releasing than OVA loaded chitosan nanoparticles, which might help to maintain OVA higher concentration in both jejunum and ileum, this probably attributed to the chitosan nanoparticles matrix erosion or degradation firstly, and the second release from cyclodextrin inclusion complexes after OVA loaded CD/CS nanoparticle transferred across tight epithelial cells to reach B cells at Peyer's Patches and induce both local and systemic immune response [32]. Overall, both the stabilization effect and the slower release profile due to cyclodextrin incorporation were responsible the increased OVA bioavailability found in OVA loaded CD/CS nanoparticle treated mice. Moreover, CD/CS nanoparticle has previously reported to be able to efficiently protect OVA and retain the protein's activity from gastric acid in stomach,

facilitating the protein absorption through nanoparticle decomposition after reaching the Peyer's patches [34]. The released OVA could reach lymphoid tissue to induce immune response [35,36]. Besides, cyclodextrin itself might trigger innate immune response at jejunum and ileum as the immunization adjuvant [37]. Overall, CD/CS nanoparticles reported herein showed great potentials as a novel oral protein delivery system to induce mucosal and systemic immune response in vivo.

4. Conclusion

A novel oral protein delivery system, OVA-loaded CD/CS nanoparticles, was successfully prepared by a precipitation/coacervation method with enhanced oral absorption, penetration and improvement of OVA stability from cyclodextrin and chitosan. The formation of OVA-CD inclusion complexes was verified by molecular docking. OVA loaded CD/CS nanoparticles had uniform particle size and exhibited higher OVA encapsulation efficiency and slower drug release rate in vitro. More importantly, in vivo evaluation results showed OVA loaded CD/CS nanoparticles could enhance its efficacy in inducing intestinal mucosal immune response. Thus, we consider that CD/CS nanoparticles can be used as a promising oral antigen delivery system to improve the immunogenicity of oral protein delivery.

Conflicts of interest

The authors report no conflicts of interest.

Acknowledgement

REFERENCES

[1] Kuolee R, Chen W. M cell-targeted delivery of vaccines and therapeutics. Expert Opin Drug Deliv 2008;5:693–702.

[2] Russell GJ. Oral vaccine delivery. J Control Release 2000;65:49–54.

[3] Fuhrmann K, Fuhrmann G. Recent advances in oral delivery of macromolecular drugs and benefits of polymer conjugation. Curr Opin Colloid In 2017;31:67–74.

[4] Jr BR, Vitale K, Sanders LM. Nafarelin controlled release injectable: theoretical clinical plasma profiles from multiple dosing and from mixtures of microspheres containing 2 per cent, 4 per cent and 7 per cent nafarelin. J Microencapsulation 2008;7:397–413.

[5] Luo YY, Xiong XY, Tian Y, et al. A review of biodegradable polymeric systems for oral insulin delivery. Drug Deliv 2016;23:1882–91.

[6] Hanns-Christian M, Stefan F, Rolph TW, Carpenter JF. Protein aggregation and particle formation: effects of formulation, interfaces, and drug product manufacturing operations. Aggreg Ther Proteins 2010;7:301–31.

[7] Liu H, Gaza-Bulseco G, Faldu D, Chumsae C, Sun J. Heterogeneity of monoclonal antibodies. J Pharm Sci 2008;97:2426–47.

[8] Samra HS, He F, Bhambhani A, et al. The effects of substituted cyclodextrins on the colloidal and conformational stability of selected proteins. J Pharm Sci 2010;99:2800–18.

[9] Tavornvipas S, Tajiri S, Hirayama F, Arima H, Uekama K. Effects of hydrophilic cyclodextrins on aggregation of recombinant human growth hormone. Pharm Res 2004;21:2369–76.

[10] Castellanos IJ, Flores G, Griebenow K. Effect of cyclodextrins on alpha-chymotrypsin stability and loading in PLGA microspheres upon S/O/W encapsulation. J Pharmacol Sci 2006;95:849–58.

[11] Kfoury M, Lounès-Hadj SA, Bourdon N, et al. Solubility, photostability and antifungal activity of phenylpropanoids encapsulated in cyclodextrins. Food Chem 2015;196:518–25.

[12] Sun Y, Gu L, Gao Y, Gao F. Preparation and characterization of 5-Fluorouracil loaded chitosan microspheres by a two-step solidification method. Chemi Pharm Bull 2010;58:891–5.

[13] Puhl S, Meinel L, Germershaus O. Recent advances in crystalline and amorphous particulate protein formulations for controlled delivery. Asian J Pharm Sci 2016;11:469–77.

[14] Dodane V, Vilivalam VD. Pharmaceutical applications of chitosan. Pharm. Sci. Technol. Today 1998;1:246–53.

[15] Xue M, Hu S, Lu Y, et al. Development of chitosan nanoparticles as drug delivery system for a prototype capsid inhibitor. Int J Pharm 2015;495:771–82.

[16] Saboktakin MR, Tabatabaee RM, Maharramov A, Ramazanov MA. Design and characterization of chitosan nanoparticles as delivery systems for paclitaxel. Carbohydr Polym 2010;82:466–71.

[17] Lubben IMVD, Verhoef JC, Aelst ACV, Borchard G, Junginger HE. Chitosan microparticles for oral vaccination: preparation, characterization and preliminary in vivo uptake studies in murine Peyer's patches. Biomaterials 2001;22:687–94.

[18] Lubben IMVD, Kersten G, Fretz MM, Beuvery C, Verhoef JC. Chitosan microparticles for mucosal vaccination against diphtheria: oral and nasal efficacy studies in mice. Vaccine 2003;21:1400–8.

[19] Chen S, Dongjun FU, Gao S, Gao F, Zuo J. Characterization and pharmacokinetics of dimethyl-β-cyclodextrin inclusion complexes of water insoluble drug BMCP25 in rats. Chin J Pharm 2013;44:171–4.

[20] Yuan Z, Ye Y, Gao F, et al. Chitosan-graft-beta-cyclodextrin nanoparticles as a carrier for controlled drug release. Int J Pharm 2013;446:191–8.

[21] Hu HY, Du HN. Alpha-to-beta structural transformation of ovalbumin: heat and pH effects. Protein J 2000;19:177–83.

[22] Furusaki E, Ueno Y, Sakairi N, Nishi N, Tokura S. Facile preparation and inclusion ability of a chitosan derivative bearing carboxymethyl-β-cyclodextrin. Carbohydr Polym 1996;29:29–34.

[23] Zhang L, Zhang Z, Li N, et al. Synthesis and evaluation of a novel β-cyclodextrin derivative for oral insulin delivery and absorption. Int J Biol Macromol 2013;61:494–500.

[24] Dotsikas Y, Kontopanou E, Allagiannis C. Interaction of 6-p-toluidinylnaphthalene-2-sulphonate with β-cyclodextrin. J Pharm Biomed Anal 2000;23:997–1003.

[25] Sakina H, Abdelaziz B, Leila N, et al. Molecular docking study on β-cyclodextrin interactions of metobromuron and [3-(p-bromophenyl)-1-methoxy-1-methylurea]. J Incl Phenom 2012;74:191–200.

[26] Liu B, Li Y, Xiao H, et al. Characterization of the supermolecular structure of polydatin/6-O-α-maltosyl-β-cyclodextrin inclusion complex. J Food Sci 2015;80:1156–61.

[27] Zhou H, Lai WP, Zhang Z, Li WK, Cheung HY. Computational study on the molecular inclusion of andrographolide by cyclodextrin. J Comput Aided Mol Des 2009;23:153–62.

[28] Hori M, Onishi H, Machida Y. Evaluation of Eudragit-coated chitosan microparticles as an oral immune delivery system. Int J Pharm 2005;297:223–34.

[29] Gao H, Wang YN, Fan YG, Ma JB. Interactions of some modified mono- and bis-β-cyclodextrins with bovine serum albumin. Bioorg Med Chem 2006;14:131–7.

[30] Slütter B, Jiskoot W. Dual role of CpG as immune modulator and physical crosslinker in ovalbumin loaded N-trimethyl chitosan (TMC) nanoparticles for nasal vaccination. J Control Release 2010;148:117–21.

[31] Suksamran T, Ngawhirunpat T, Rojanarata T, et al. Methylated N-(4-N,N-dimethylaminocinnamyl) chitosan-coated electrospray OVA-loaded microparticles for oral vaccination. Int J Pharm 2013;448:19–27.

[32] Facciuolo A, Gonzalez-Cano P, Napper S, Griebel PJ, Mutharia LM. Marked differences in mucosal immune responses induced in ileal versus jejunal peyer's patches to mycobacterium avium subsp. paratuberculosis secreted proteins following targeted enteric infection in young calves. PLos One 2016;11:e0158747.

[33] Kamphorst AO, Am MDSI, Sinisterra RD. Association complexes between ovalbumin and cyclodextrins have no effect on the immunological properties of ovalbumin. Eur J Pharm Biopharm 2004;57:199–205.

[34] Kreuter J. Nanoparticles and microparticles for drug and vaccine delivery. J Anat 1996;189:503–5.

[35] Barackman JD, Singh M, Ugozzoli M, Ott GS, O'Hagan DT. Oral immunization with poly(lactide-co-glycolide) microparticles containing an entrapped recombinant glycoprotein (gD2) from herpes simplex type 2 virus. S.t.p.pharma Pratiques 1998;8:41–6.

[36] Marttin E, Verhoef JC, Spies F, et al. The effect of methylated β-cyclodextrins on the tight junctions of the rat nasal respiratory epithelium. J Control Release 1999;57:205–13.

[37] Onishi M, Ozasa K, Kobiyama K, et al. Hydroxypropyl-β-cyclodextrin spikes local inflammation that induces Th2 cell and T follicular helper cell responses to the coadministered antigen. J Immunol 2015;194:2673–82.